RESEARCH ARTICLE | JANUARY 18 2024

# A new application of the boundary element method to compute the single-scattering properties of complex ice crystals in the microwave FREE

Anthony J. Baran ✉; Antigoni Kleanthous; Timo Betcke; David Hewett; Christopher Westbrook



*AIP Conf. Proc.* 2988, 040001 (2024)
https://doi.org/10.1063/5.0183478

# A New Application of the Boundary Element Method to Compute the Single-Scattering Properties of Complex Ice Crystals in the Microwave

Anthony J. Baran[1,2, a)], Antigoni Kleanthous[3], Timo Betcke[3], David Hewett[3], and Christopher Westbrook[4]

[1]*Met Office, Exeter, Devon, UK*
[2]*University of Hertfordshire, Department of Physics, Astronomy, and Mathematics, Hatfield, UK*
[3]*University College London, Department of Mathematics, London, UK*
[4]*University of Reading, Department of Meteorology, Reading, UK.*

[a)] Corresponding author: anthony.baran@metoffice.gov.uk

**Abstract.** The Boundary Element Method (BEM) is being applied to compute the single-scattering properties of randomly oriented complex rosette ice aggregates at the frequencies of 50, 183, 243 and 664 GHz, for the temperatures 190, 230, and 270 K. The rosette aggregates were generated using a Monte Carlo model, and from the statistical runs, 65 aggregates were selected that were within ±30% of an existing mass–dimension relation that is consistent with the Met Office's cirrus microphysics scheme in its weather and climate models. The generated 65 aggregates have maximum dimensions between 10 μm and approximately 1 cm. To compute efficiently their single-scattering properties using BEM, random orientation is approximated by rotating the incident wave about the scatterer rather than the other way around as is done in all other electromagnetic methods. This exploits the BEM linear matrix equation (i.e. **Ax**=**b**) by only needing to compute the matrix **A** once, leaving the less computationally demanding **b** to change. We show that our representation of random orientation can accurately compute the single-scattering properties of non-axisymmetric particles to within 1 or 2% of T-matrix solutions, and we compare the solutions found for our rosette aggregate models with other commonly used models in the microwave.



## INTRODUCTION

With the launch of the space-based Ice Cloud Imager (ICI) in 2025 that will observe cirrus and ice cloud between 183 and 664 GHz, and some channels will simultaneously measure the vertical and horizontal polarizations, it is important to improve the representation of ice crystal scattering and absorption in weather and climate models. This will enable better assimilation of ICI data in weather models to improve their prediction of extreme weather events. However, currently employed single-scattering properties in weather and climate models are not consistent in the sub-mm regions of the electromagnetic spectrum [1, 2]. To improve on this situation, we apply BEM to compute efficiently the single-scattering properties (SSPs) of randomly oriented rosette aggregates by applying accelerated matrix solving techniques that reduce the memory costs and solution times of BEM by 99 and 75%, respectively, and this being especially so at the highest size parameters [3, 4]. The SSPs of the rosette aggregates are based on models that have consistent masses and orientation-projected areas found in naturally occurring cirrus and ice cloud [5], as well as the assumed mass–dimension relation in the cirrus microphysics scheme in a weather model. This important consistency condition is lacking in the cirrus scattering models used in the studies by [1, 2]. Only by generating consistent scattering models that are linked to observed properties can we improve the predictive quality of weather and climate models across the electromagnetic spectrum of importance to these models.

*Radiation Processes in the Atmosphere and Ocean*
AIP Conf. Proc. 2988, 040001-1–040001-5; https://doi.org/10.1063/5.0183478
Published by AIP Publishing. 978-0-7354-4779-0/$30.00

## The rosette aggregate ice models

Here, we exploit the recent observations by [5], which showed that within in-situ generated cirrus, typical of the mid-latitudes, budding rosettes and rosette aggregates contributed the most to their observations of ice crystal mass and area. To follow these observations, we use the Monte Carlo model developed by [6] to generate the budding rosettes and rosette aggregates, which includes realistic fall speeds of the individual monomers that make up the aggregates. Moreover, to be consistent with the Met Office's ice microphysics scheme, the mass–dimension relation of the generated aggregates must be within ±30% of the same relation used in the previous scheme. This ensures consistency between the SSPs and the ice microphysics scheme. Figure 1 shows how well the generated budding rosettes and rosette aggregates follow the assumed mass–dimension relation, along with some images of the model shapes.

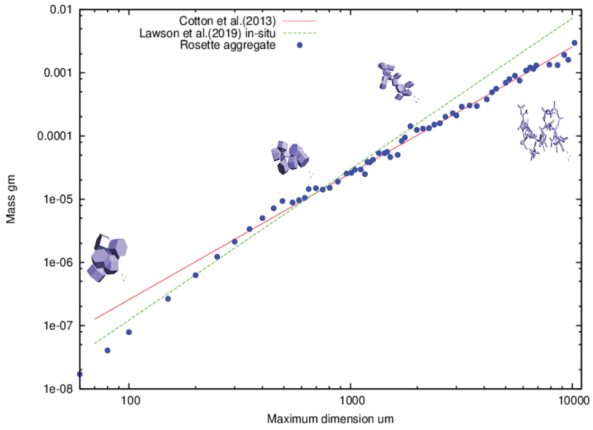


**FIGURE 1.** The mass plotted against the ice crystal maximum dimension, where in the figure the budding rosettes and rosette aggregate results, the assumed and observed mass–dimension relations are defined by the key at the top left of the figure. Also shown are some images of the budding rosettes and rosette aggregate models.

As it can be seen from the figure, the rosette aggregate models follow the assumed mass–dimension relation from [7] very well. At a size of 492 μm the budding rosettes are scaled down to 10 μm, and these particles have mass proportional to $D_{max}^{3.0}$, where $D_{max}$ is the maximum dimension of the ice crystal. However, the rosette aggregates have mass = $0.0257D_{max}^{2.0}$ [7]. Note here that the budding rosettes tend to follow the observed mass–dimension [5] more closely at the smaller maximum dimensions. As the ice crystals become more aggregated, the images embedded within Fig. 1 become more spatial as observed [5, 7].

## The representation of random orientation within the framework of BEM

The advantages of BEM, also known as the Method of Moments, to compute the SSPs of complex ice crystals are that it reformulates the Maxwell equations as integrals on the boundary, thus reducing the problem from 3D to 2D. The solutions found on the boundary can be extended to the interior, exterior, or far-field via the Stratton-Chu representation formulae. Moreover, the radiation condition at infinity is automatically satisfied, and any complex particle shape can be solved for if they obey the condition of Lipschitz continuity. Upon applying Galerkin discretization to the boundary integral equations, a linear matrix equation of the form $\mathbf{Ax}=\mathbf{b}$ is derived by [3, 4]. Here, $\mathbf{A}$ is the large matrix of the linear system, which contains the integral operators comprising the electric and magnetic potentials, scattering geometry, refractive index, the size parameter, and the wavenumbers of the incoming waves. The vector $\mathbf{b}$ just contains information on the direction and polarization of the incident wave, so $\mathbf{b}$ is much less computationally demanding than the matrix $\mathbf{A}$, and $\mathbf{A}$ is dense and usually ill-conditioned. However, as previously mentioned [3, 4] found a particular preconditioning of the linear system that reduced the memory costs and solution times substantially. This accelerated solution technique is applied in this article.

The method adopted here for random orientation is fully explained in [8], but a brief explanation is given here. Traditionally, to find the scattered field the incident wave is kept fixed at some polar and azimuthal angle, but the scatterer is rotated about the three Eulerian angles (α, β, γ). In [8], it is shown that equivalent random orientation can

be achieved if the scatterer is kept fixed, but the incident wave is rotated about the scatterer. This method of equivalent random orientation takes advantage of the equation **Ax**=**b** because **b** contains the directional information and **A** need only be computed once. To solve for the SSPs using BEM, we need to specify the discretization of the boundary (or how many elements per incident wavelength), the number of incident waves and the number of polarization directions. Note here, the number of polarization directions depends on the polar, azimuthal and $\gamma$ angles, but the number of incident waves depends only on the polar and azimuthal angles, which in the traditional framework is equivalent to ($\alpha$, $\beta$). To test our representation of random orientation and the number of elements per wavelength, the numbers of incident waves, and polarization directions required to solve for the SSPs of a particular case, we use the randomly oriented hexagonal ice column of aspect ratio unity of size parameter 10 (i.e. $\pi D_{max}/\lambda$) as an example. The resulting comparisons are presented in Fig. 2 (a) and (b).

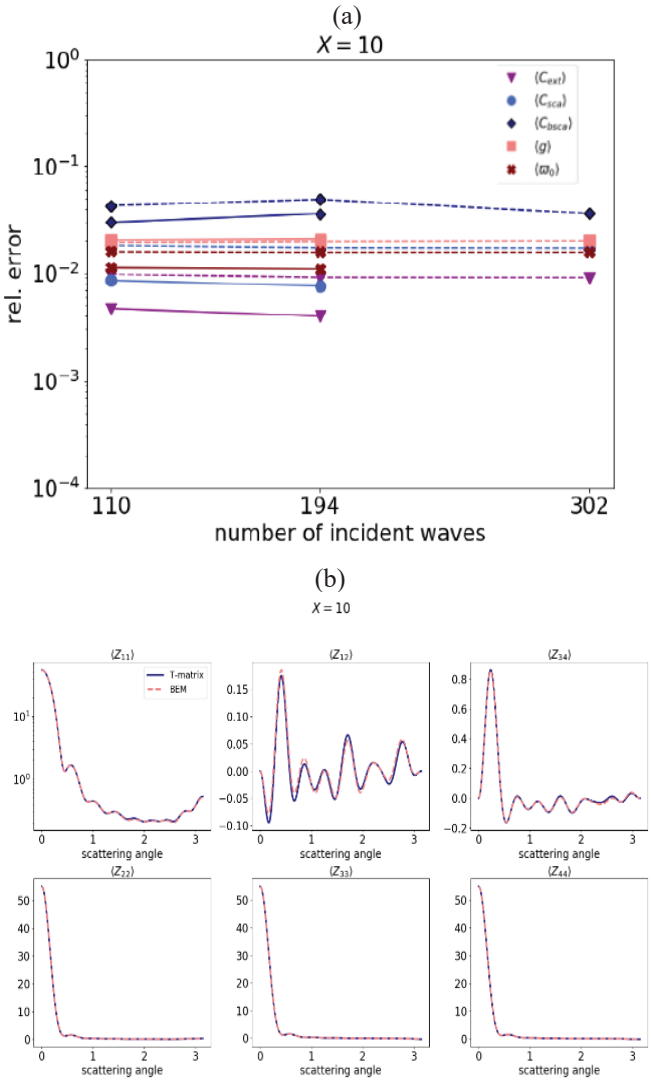


**FIGURE 2.** (a) Relative error between the BEM and T-matrix solutions found for the total optical properties plotted against the number of incident waves. The dashed and full lines assume a discretization of 10 and 20 elements per wavelength, respectively. The key to the figure is shown at the top right. (b) Solutions found for the phase matrix plotted against scattering angle using T-matrix (full blue line) and BEM (dashed red line) assuming a discretization of 20 elements per wavelength.

As it can be seen from Fig. 2(a), the industry rule of thumb of applying 10 elements per wavelength to obtain accurate solutions using BEM is not general, since improved agreement between BEM and T-matrix [9] is found

using a discretization of 20 elements per wavelength. This is particularly important for smaller size parameters, where a sufficient discretization of the boundary might not be achieved with 10 elements per wavelength. We also note that after 194 incident waves, the solutions relative to T-matrix do not vary much. In general, the BEM solutions are seen to be within a few percent of the T-matrix solutions. This level of accuracy is sufficient for atmospheric physics. We see that in Fig. 2 (b) that assuming 194 incident waves and a discretization of 20 elements per wavelength, the BEM solutions found for the phase matrix agree very well with the T-matrix solutions. In this case, the number of polarization directions is 15 to obtain the agreement seen in Fig. 2 (b). In the case of the $Z_{12}$ element, there is some slight disagreement between the two methods, but this could be resolved by increasing the number of elements per wavelength in the case of BEM. In [8] it is found that the number of elements required, and numbers of incident waves and polarization directions depends on the size parameter and particle complexity. This requires some experimentation to obtain BEM accuracies to be within the acceptable accuracy of a few percent.

## Comparisons with other models in the microwave

In this section, we compare the scattering and absorption coefficients obtained using BEM applied to all 65 rosette models and compare these with other models at the frequency of 243 GHz at a temperature of 190 K. The frequency of 243 GHz is chosen because this frequency has been shown to be particularly sensitive to ice crystal shape by [10]. Other scattering properties are not shown here for reasons of brevity. In the study by [10] it was also shown that the long-column aggregate model developed by [11] best minimized differences between radiative transfer simulations and measurements over some microwave and sub-mm frequencies. Moreover, the compact eight-column hexagonal aggregate also described in [11] was shown by [10] to provide the worst agreement between model simulations and measurements. Finally, the six-branched rosette was also shown by [10] to give similar results to the long-column aggregate. The results of these comparisons are presented in Fig. 3 (a) and (b).

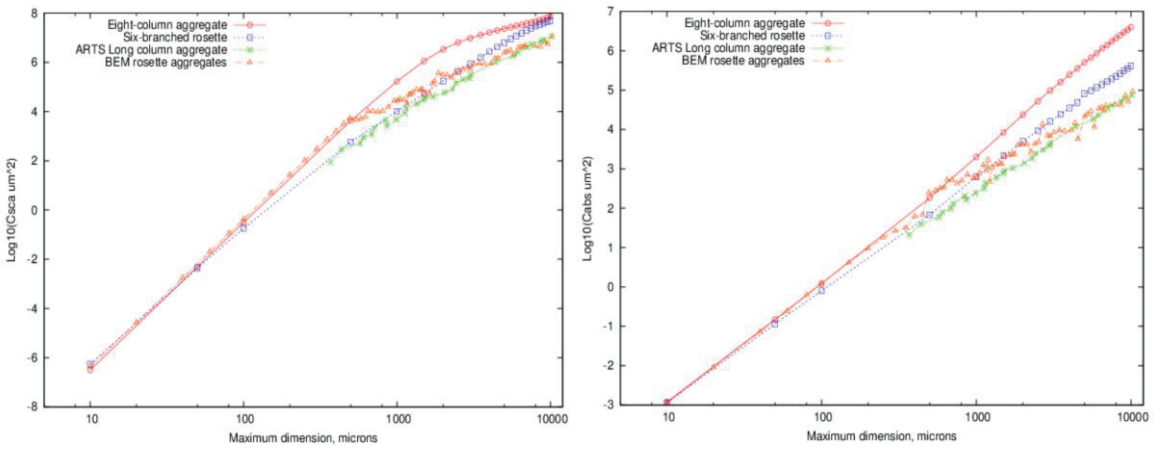


(a) (b)

**FIGURE 3.** (a) The common logarithm of the scattering coefficient plotted against the ice crystal maximum dimension. (b) The same as (a) except for the absorption coefficient. The key to both (a) and (b) is shown at the top left.

The important point about Fig. 3 is that the BEM ice crystal model shows the significant transition between the budding rosettes and the rosette aggregates at approximately 492 μm, the transition between mass proportional to $D_{max}^3$ and $D_{max}^2$ particles. This transition is not evident in any of the other models. Moreover, at $D_{max} > 492$ μm, the rosette aggregate solutions rapidly move away from the compact eight-column hexagonal aggregate to the other models, and at the largest sizes are like the long column aggregate model. At $D_{max} < 100$ μm, the solutions tend to be similar as would be expected because the size parameter tends towards the limit of Rayleigh scattering at 243 GHz.

## CONCLUSION

In this article, we have presented a synopsis of BEM applied to very complex ice particles. The adopted model of budding rosettes and rosette aggregates is based on observations, and the models have been generated using a Monte Carlo aggregation model that has realistic fall speeds of individual monomers that make up the aggregate. Moreover, the model has a natural transition in mass between the mass proportional to $D_{max}^3$ and $D_{max}^2$ particles, unlike other scattering models, which do not. Furthermore, the rosette aggregate models follow an assumed mass–dimension relation that is consistent with the microphysics in a weather and climate model, to ensure that the SSPs are consistent with the ice microphysics assumptions in the cloud schemes of the models. It has also been shown that BEM can replicate solutions found for the randomly oriented hexagonal ice column using T-matrix, but the accuracy of the BEM solutions depends on the number of elements per wavelength, the numbers of incident waves and polarization directions. These in turn are size parameter dependent. Currently, the database of microwave and sub-mm SSPs for the budding rosettes and rosettes aggregates is being prepared and should be available in early 2023 for the atmospheric physics community to utilize. The model will be extended in due course across the electromagnetic spectrum of relevance to weather and climate models.

## REFERENCES


1. R. J. Bantges et al., Atmos. Chem. Phys, **20**, 12889-12903 (2020).
2. S. Fox et al., Atmos., Meas., Tech, **12**, 1599-1617 (2019).
3. A. Kleanthous et al., J. Quant. Spectros. Radiat. Transf, **224**, 383-395 (2019).
4. A. Kleanthous et al., J. Comp. Phys, **458**, 111099 (2022).
5. R. P. Lawson et al., J. Geophys. Res, **124**, 10049-10090 (2019).
6. C. D. Westbrook et al., Phys. Rev. E, **70**, 021403 (2004).
7. R. J. Cotton et al., Quart. Jour. Roy. Met. Soc, **139**, 1923-1934 (2013).
8. A. Kleanthous et al., Remote Sens, in preparation, (2022).
9. S. Havemann and A. J. Baran, J. Quant. Spectros. Radiat. Transf, **70**, 139-158 (2001).
10. S. Fox, Remote Sens, **12**, 2758 (2020).
11. P. Eriksson et al., Earth Syst. Sci. Data, **10**, 1301-1326 (2018).